Overview of HZETRN and BRNTRN space radiation shielding codes

John W. Wilson, F. A. Cucinotta, J. L. Shinn, and L. C. Simonsen

NASA Langley Research Center MS 236
Hampton, VA 23681-0001
Tel: 804 864 4635, Fax: 804 864 7607, email:a.w.burner@larc.nasa.gov

F. F. Badavi

Christopher Newport University, Newport News, VA 23601

ABSTRACT

The NASA Radiation Health Program has supported basic research over the last decade in radiation physics to develop ionizing radiation transport codes and corresponding data bases for the protection of astronauts from galactic and solar cosmic rays on future deep space missions. The codes describe the interactions of the incident radiations with shield materials where their content is modified by the atomic and nuclear reactions through which high energy heavy ions are fragmented into less massive reaction products and reaction products are produced as radiations as direct knockout of shield constituents or produced as de-excitation products in the reactions. This defines the radiation fields to which specific devices are subjected onboard a spacecraft. Similar reactions occur in the device itself which is the initiating event for the device response. An overview of the computational procedures and data base with some applications to photonic and data processing devices will be given.

Key words: cosmic rays, ionizing radiation, shielding

1. INTRODUCTION

The Langley Research Center has a longstanding collaborative program of theoretical/experimental physics of heavy ions. The research treats interaction with materials at three levels: (1) at the level of interactions between the radiation and the atomic constituents (electrons and nuclei), (2) at the microscopic level of radiation transport and energy deposition processes in sensitive structures, and (3) at the level of testing and demonstrating the applicability of the theory to completed experiments and to supporting new, more precise experiments on limiting important components. The results of this research must enable the prediction of the complex mixture of radiations within the space structures and devices due to every important environmental component to which exposure is made and allow experimental verification to high accuracy of those predictions in controlled laboratory simulations and instrumented flight experiments.

2. TRANSPORT THEORY

The relevant transport equations are derived on the basis of conservation principles[1] for the flux density $\phi_j(x,\Omega,E)$ of type j particles as

$$\Omega\cdot\nabla\phi_j(x,\Omega,E)=\sum_k\int\sigma_{jk}(\Omega,\Omega',E,E')\phi_k(x,\Omega',E')d\Omega'dE'-\sigma_j(E)\phi_j(x,\Omega,E) \tag{2.1}$$

where $\sigma_j(E)$ and $\sigma_{jk}(\Omega,\Omega',E,E')$ are the media macroscopic cross sections. The $\sigma_{jk}(\Omega,\Omega',E,E')$ represent all those processes by which type k particles moving in direction Ω' with energy E' produce a type j particle in direction Ω with energy E. Note that there may be several reactions which produce a particular product, and the appropriate cross sections for equation (2.1) are the inclusive ones. The total cross section $\sigma_j(E)$ with the medium for each particle type of energy E may be expanded as

$$\sigma_j(E)=\sigma_j^{at}(E)+\sigma_j^{el}(E)+\sigma_j^{r}(E) \tag{2.2}$$

where the first term refers to collision with atomic electrons, the second term is for elastic nuclear scattering, and the third term describes nuclear reactions. The microscopic cross sections and average energy transfer are ordered as follows:

$$\sigma_j^{at}(E) \sim 10^{-16} \text{ cm}^2 \text{ for which } \Delta E_{at} \sim 10^2 \text{ eV} \tag{2.3}$$

$$\sigma_j^{el}(E) \sim 10^{-19} \text{ cm}^2 \text{ for which } \Delta E_{el} \sim 10^6 \text{ eV} \tag{2.4}$$

$$\sigma_j^{r}(E) \sim 10^{-24} \text{ cm}^2 \text{ for which } \Delta E_{r} \sim 10^8 \text{ eV} \tag{2.5}$$

This ordering allows flexibility in expanding solutions to the Boltzmann equation as a sequence of physical perturbative approximations. It is clear that many atomic collisions (~10^6) occur in a cm of ordinary matter, whereas ~10^3 nuclear coulomb elastic collisions occur per cm. In distinction, nuclear reactions are separated by a fraction to many cm depending on energy. Special problems arise in the perturbation approach for neutrons for which, $\sigma_n^{at}(E) \approx 0$ and the nuclear elastic process appears as the first-order perturbation.

As noted in the development of equation (2.1), the cross sections appearing in the Boltzmann equation are the inclusive ones so that the time-independent fields contain no spatial (or time) correlations. However, space- and time-correlated events are functions of the fields themselves and may be evaluated once the fields are known[2]. Such correlations are important to the biological injury of living tissues. For example, the correlated release of target fragments in biological systems due to ion or neutron collisions have high probabilities of cell injury with low probability of repair resulting in potentially large RBE and quality factor[1,3]. Similarly, the correlated release of secondary electrons in atomic collisions with the massive ions leads to important features in biological response as well as in active regions within electronic devices[4,5,6].

The solution of equation (2.1) involves hundreds of multi-dimensional integro-differential equations which are coupled together by thousands of cross terms and must be solved self-consistently subject to boundary conditions ultimately related to the external environment and the geometry of the astronaut's body and/or a complex vehicle. The early computations were made using the atomic interaction as the first perturbation term (equation 2.3) and neglecting the higher-order perturbations. The mean energy loss was introduced in a continuous slowing down approximation (csda), and straggling was neglected for the broad energy spectra of the space radiations but was important in the nearly monoenergetic laboratory experiments[7].

The second perturbation term (equation 2.4) is generally dominated by the highly directional coulomb cross section for charged ions and nuclear elastic scattering for neutrons. The coulomb scattering has negligible effects on the nearly isotropic and uniform space radiations[8] but is of great importance to the nearly unidirectional and nearly point source laboratory beams. The angular dispersion and its effects on lateral beam spread and range straggling are important corrections in comparing to laboratory measurements[7]. The nuclear elastic scattering is especially important to neutron fields and has been treated in the past using Monte Carlo methods[9] and multigroup methods[10]. Any other method requires compromise, and Monte Carlo provides a good test bed for approximate procedures. However, due to the poor computational efficiency, Monte Carlo methods will always have limited usefulness but multigroup methods hold promise for efficient space engineering applications[10].

The third perturbation term consists of complex energy and angle functions for which Monte Carlo was the first approach. Results from these Monte Carlo codes provided the basis of the generation of analytical techniques and the simplification of boundary conditions which have had an enormous impact on space shield code development[1,8,11].

2.1. Transport coefficients

The transport coefficients relate to the atomic/molecular and nuclear processes by which the particle fields are modified by the presence of a material medium. As such, basic atomic and nuclear theories provide the input to the transport code data base. It is through the nuclear processes that the particle fields of different radiation types are transformed from one type to another. The atomic/molecular interactions are the principal means by which the physical insult is delivered to biological systems in producing the chemical precursors to biological change within the cells. The temporal and spatial distributions of such precursors within the cell system governs the rates of diffusive and reactive processes leading to the ultimate biological

effects. Similarly these atomic processes are responsible for the excess ionization within optical sensitive and signal processing devices resulting in spurious signals.

2.1.a. Atomic/Molecular Interactions. The first order physical perturbation to the right side of equation (2.1) is the atomic/molecular cross sections as noted in equation (2.3) for which those terms in (2.1) are expanded about the energy moments as

$$S_n(E) = \sum_i \varepsilon_i^n \sigma_i(E) \tag{2.6}$$

where ε_i is based on the electronic excitation energy, and $\sigma_i(E)$ is the total atomic/molecular cross section for delivering ε_i energy to the orbital electrons (including discrete and continuum levels). The first moment (n = 1) is the usual stopping power, and the usual continuous slowing down approximation (csda) is achieved by neglecting the higher-energy moments. The second energy moment is related to range straggling and provides corrections to the ion slowing down spectrum[1]. Equation (2.6) is misleadingly simple since specification of ε_i and $\sigma_i(E)$ require a complete knowledge of the atomic/molecular wave functions. A many body local plasma model has been found useful in approximating the atomic and molecular quantities for the positive energy moments[12]. The current stopping power data base is derived semiempirically as the Bethe reduction of equation (2.6) in terms of mean excitation energies and shell corrections[1]. The usual relativistic correction and density effect correction of Sternheimer are included[13]. The straggling effects of the second energy moment will be included in the near future[1,12].

The passing ions are not the primary mediators of biological injury, but rather the secondary electrons generated in atomic collisions which transport the energy lost by the passing ion to the biological medium. The distribution of the electrons about the ion path is critical to evaluation of biological injury[4,5], are critical to the evaluation of shield attenuation properties[14], and fundamental to evaluation of effects in active electronic devices[6]. Such effects are likewise governed by equation (2.1). The secondary electrons are treated using the electron source terms of Rudd[15] and the electron propagation methods of Dupouy et al.[16] as modified by Kobetich and Katz[17] and recently improved by Cucinotta et al.[4].

The next physical perturbation term is the coulomb scattering by the atomic nucleus and is represented by Rutherford scattering modified by screening of the nuclear charge by the orbital electrons using the Thomas-Fermi distribution for the atomic orbitals. The total nuclear coulomb cross section found by integrating over the scattering directions is related to the radiation length. The differential cross section is highly peaked in the forward direction, and only after many scatterings is significant beam divergence seen. We will follow the lead of Schimmerling and co-workers in implementing Fermi's solution to a restricted Boltzmann equation in which the first physical perturbation terms are neglected[7].

2.1.b. Nuclear Interactions. The extent of the nuclear interaction cross section data base required for the transport of cosmic rays spans most nuclear-reaction physics from thermal energies to energies above tens of GeV/amu, including a large number of projectile and target material combinations. The types of cross sections required for the transport involve total yields and secondary energy spectra for one-dimensional transport and double differential cross sections in angle and energy for three-dimensional transport. Fortunately, neutron and proton cross sections have been studied at some length in the past. Nuclear-reaction modeling is required, especially for light and heavy ion projectiles, to understand the basic physical processes, and to extrapolate the limited, available experimental data between projectile energies and projectile-target combinations.

Microscopic Theory. A microscopic theory for the description of nuclear fragmentation is being developed through the study of the summation of the nucleus-nucleus, multiple-scattering series for inclusive reactions where a single reaction species is considered. This approach originated in a theory for high energy alpha particle fragmentation[18] and has been extended to recast the abrasion-ablation model in microscopic form[19]. The microscopic theory can be shown[19] to reduce to the optical-model formulation of abrasion[20] which in turn reduces to the geometric abrasion model[21]. The microscopic theory represents a unified approach where a single formalism generates all production cross sections required for heavy ion transport. We note that previously the production of heavy fragments, light ions, and nucleons were treated separately, often with disjoint assumptions[22]. A unified approach will be useful because the production spectrum of nucleons and light ions from abrasion correlates directly with the formation of pre-fragment nuclei and their excitation spectra.

The microscopic approach proceeds by formulating the multiple-scattering series for heavy ion reactions in terms of response functions for an arbitrary number of particle knockouts, appropriate for inclusive reaction theory, and generalized to the case of heavy ion abrasion dynamics[19]. The reaction dynamics for fragmentation processes are then unified by the development of a single function, the multiple scattering amplitude, in terms of the momentum vectors of all secondary reaction products. The reaction cross sections for the various secondaries are then found by considering the phase space for an arbitrary final state where there are n abraded particles, leaving a projectile pre-fragment with energy denoted E_F^*. Conserving energy in the pre-fragment formation when all interactions with the target are complete, the scattering amplitude f_{fi} and cross sections are related by

$$d\sigma = \sum_X \prod_{j=i}^{n} \left[\frac{d\vec{k}_j}{(2\pi)^3} \right] \delta\left(E_i - E_f\right) dE_F \cdot d^2q \left| f_{fi} \right|^2 \tag{2.7}$$

where the $\vec{k}$ are the abraded nucleon wave vectors, E_i and E_f are the energies in the initial and final states, and q is the total transverse momentum in the reaction. Equation (2.7) is summed over the final states of the target nuclei in which $\vec{q} = \vec{P}_T - \vec{P}_X$. In the abrasion-ablation model there is a causal assumption that separates the time evolution of ablation processes from the abrasion. It follows that for the emission of ν nuclei from the excited pre-fragment with energies E_r we have $E_F^* = E_F + \sum_{r=0}^{\nu} E$ where $\nu = 0$ is allowed in order to include the possibility that the pre-fragment excitation energy is below the lowest particle-emission channel. The inclusive nucleon momentum distribution is found from equation (2.7) for the abraded particles as

$$\frac{d\sigma}{d\vec{k}_{j=1}} = \sum_n \sum_X \int \prod_{j=2}^{n} \left[\frac{d\vec{k}_j}{(2\pi)^3} \right] \int d^2q dE_F \cdot \delta\left(E_i - E_f\right) \left| f_{fi} \right|^2 \tag{2.8}$$

where we are integrating over all kinematical variables except the momentum of one abraded particle. The excitation spectra of the pre-fragment nuclei are also obtained from equation (2.7) as

$$\frac{d\sigma_n}{dE_F \cdot} = \sum_X \int \prod_{j=i}^{n} \left[\frac{d\vec{k}_j}{(2\pi)^3} \right] \int d^2q \delta\left(E_i - E_f\right) \left| f_{fi} \right|^2 \tag{2.9}$$

The decay of the pre-fragment nuclei into the final fragment opens the kinematical phase space further, and this description will be required for predicting the final mass yields as well as the momentum distribution of ablated nucleons or nuclei.

The description of the development of the scattering amplitude in terms of abrasion response functions has been made using the eikonal model. The many body response functions are being developed as convolutions of one-body response functions using the shell model and a correlated Fermi gas model. The corrections to the eikonal theory are then well known and include large angle scattering corrections and the many body effects contained in the full nuclear propagator. Ablation can then be described by well known statistical and resonance theories for nominal pre-fragment excitation energies with new phenomenon possibly occurring for extremely large values in the excitation energy spectrum.

Quantum Mechanical, Optical Potential, Abrasion-Ablation-FSI Model. If one assumes closure on the prefragment's quantum states and neglects energy conservation in the microscopic theory, the energy-dependent, quantum-mechanical, optical potential, abrasion model[20] is obtained. The model is a quantum-mechanical abrasion (nucleon removal) formalism to describe the formation of an excited prefragment which decays (ablates) by emission of nucleons and composites (e.g., alphas) to become the final fragment. The ablation step is currently modeled using the EVA-3 Monte Carlo, cascade-evaporation computer code. The abrasion model uses actual nuclear densities extracted from electron-scattering data and incorporates energy-dependent two-nucleon transition amplitudes obtained from experiment. The goal is to complete the packaging of the current model as a self-contained, user-friendly computer code (named OPTFRG) for use in generating fragmentation cross section data bases.

Semiempirical Fragmentation Model. If one replaces the quantum mechanical abrasion cross sections by those for nuclei represented as partially transparent uniform spheres and a semiempirical correction to the surface energy to correct the

prefragment excitation energy when the prefragment is far from equilibrium, then one obtains the semiempirical fragmentation model. It is a highly efficient fragmentation data-base code and can represent available experimental data[23], even at relatively low energies when coulomb trajectory corrections are made. It is not as fundamental a code as the microscopic theory because it is limited by the semiempirical correction and by the assumption that nuclei are uniform spheres. This code will be modified to include target knockout, fragment contributions, and meson production.

2.2. Transport Solution Methods

The solution to equation (2.1) can be written in operational form as $\phi = G\phi_B$ where ϕ_B is the inbound flux at the boundary, and G is the Green's function which reduces to a unit operator on the boundary. A guiding principle in radiation-protection practice is that if errors are committed in risk estimates, they should be overestimates. The presence of strong scattering terms in equation (3.1) provides lateral diffusion along a given ray. Such diffusive processes result in leakage near boundaries. If $\phi_\Gamma(\Gamma)$ is the solution of the Boltzmann equation for a source of particles on the boundary surface Γ, then the solution for the same source on Γ within a region enclosed by Γ' denoted by $\phi_\Gamma(\Gamma)$ has the property

$$\phi_{\Gamma'}(\Gamma) = \phi_\Gamma + \varepsilon_{\Gamma'} \tag{2.10}$$

where $\varepsilon_{\Gamma'}$ is positive provided Γ' completely encloses Γ. The most strongly scattered component is the neutron field for which $\varepsilon_{\Gamma'} \approx 0.2$ percent for infinite media for most practical problems[8,24]. Standard practice in space radiation protection replaces G as required at some point on the boundary and along a given ray by the corresponding G_N evaluated for normal incidence on a semi-infinite slab. The errors in this approximation are second order in the ratio of beam divergence and radius of curvature of the object[8], rarely exceed a few percent for space radiations, and are always conservative. The replacement of G by G_N as a highly accurate approximation for space applications has the added advantages that G_N is the natural quantity for comparison with laboratory simulations and has the following properties: If G_N is known at a plane a distance x' from the boundary (assumed at the origin), then the value of G_N at any plane $x \geq x'$ is

$$G_N(x) = G_N(x - x')G_N(x') \tag{2.11}$$

Setting $x = x' + h$ where h is small and of fixed-step size gives rise to the marching procedures of HZETRN. Allowing $x - x'$ to take arbitrary values gives rise to the nonperturbative methods. The primary difference between the two methods is the numerical implementation. The marching procedure (HZETRN) is simple[1] and straightforward while the nonperturbative methods (GRNTRN) require some subtle analysis[25,26,27]. The freedom to take arbitrarily large steps as opposed to many small steps holds great promise for vastly improved computational efficiency.

3. TRANSPORT CODE VALIDATION

In laboratory experiments, the primary particle beam is reasonably defined with simple boundary conditions, and it is the atomic/nuclear transport properties and solution techniques that are primarily tested. There are two very useful types of detection systems with which to compare the transport models. The first is the advanced particle detector techniques of the LBL group under Jack Miller[28]. The primary particle beam is incident on the target material being tested, and the transmitted fluence is measured by particle detectors and energy discriminators. The first comparisons (figure 1) were with 600 MeV/amu Fe-56 beam on a 2 cm polyethylene target[29] using the GRNTRN code and was largely responsible for recent improvements in the NUCFRG2 database generator code[29]. Also used in code improvement were the measurements of Dr. E. V. Benton using plastic nuclear track detectors (PNTD's). Exposures of PNTD's were made to 525 MeV/amu Fe beams behind aluminum or polyethylene degraders of various thicknesses. These comparisons required an accurate representation of the experimental beam line using a multilayered Green's function code developed for these comparisons[30]. Further comparison with the C, N, and O transport measurements at GSI have shown the importance of nuclear clustering effects in alpha removal. The contributions of cluster knockout to the internal environment has been tested in measurements by Badhwar[31] as shown in figure 2. Further improvements in the nuclear database is shown based on the knockout cross sections. There is still ambiguity in the knockout spectra as studied by Cucinotta[32]. The alpha removal cross section for O projectiles shows strong target and energy dependence as shown in figure 3. Accurate cluster wave functions are required for these calculations and

future efforts and a corresponding measurements program on cluster knockout is necessary to assure the validity of the final models.

Comparison of models with spaceflight experiments is an integrated test of external environmental models, transport through realistic shielding, and prediction of detector response. Generally, the instrumentation in spaceflight is simplified (TLD, TEPC, PNTD), and the detector response is not always well-known. A response model of the TEPC is under development[2,6] and will be able to treat the problem of stopping ions (enders), straggling, and track width. Track-structure including the wall effects, is yet to be modeled. Even the PNTD detectors response depends on how they are processed and the comparison of predicted response and measured response[33] are in reasonable agreement for the D1 mission of Spacelab as shown in figure 4. Note that the LET spectra can be quite different from the measured values as shown in the figure. Further validation of the nuclear database shows that the event multiplicities for Fe beams in nuclear emulsion are in reasonable agreement with the results of NUCFRG2 code whereas the fireball like models overpredict the low multiplicities and grossly underpredict the high multiplicity events[34]. Still there are systematic model errors in the NUCFRG2 model resulting from the use of the spherical density distributions of the nucleon density[29].

4. CURRENT CODE STATUS

The evaluation of radiation risks to astronauts is always tentative and estimating the uncertainties is to a degree unclear. There is now a fair track record on the estimated attenuation properties of dose equivalent behind aluminum shielding (fig. 5). In that the more recent calculations (NUCFRG2, soft and hard spectrum) were for a different GCR environmental model we show the attenuation of NUCFRG2, soft spectrum, and hard spectrum scaled to the peripheral limit values of the new GCR environment for which the major differences between the curves in figure 5 is due to the nuclear cross sections and the nature of the transport calculation. The central and peripheral limits are based on the unitarity limits of the projectile fragmentation states without cluster knockout events. The Letaw et al. code[35] uses the Silberberg-Tsao cross sections which we found as underestimates in comparing to Schimmerling's data for Ne beams at the Bevalac[22]. The NUCFRG1 code was the first Langley fragmentation database fit to the atmospheric airshower data[36]. NUCFRG2 is the revised code fit to the last experiments of the Bevalac using Fe beams. The soft and hard spectrum is the uncertainty in the knockout spectra for the revised physical model derived by Cucinotta based on comparison to the shuttle data. It is clear that the attenuation properties of aluminum shielding have changed drastically over the last few years. Although we presume we are in a converging process it is difficult to project the final outcome since new physical processes (e.g., mesons, muons, electromagnetic cascades, etc.) are being added and validation is a slow and tedious task. Our current best estimates lie somewhere between the hard and soft spectral results.

The mainline codes (GRNTRN and HZETRN) at LaRC all use the csda stopping cross sections and ignore straggling and multiple scattering. Multiple-scattering corrections are made to the nonperturbative GRNTRN at the time of comparison with experiments using Schimmerling's method[7]. Both transport codes use the energy dependent NUCFRG2 code augmented with the Silberberg-Tsao model for hydrogen targets[37]. HZETRN and GRNTRN (to second order) allow nuclear cross-section variation along the ion path. Target fragments from nucleon and light particles ($Z \leq 2$) are transported in HZETRN but not in GRNTRN. Only space radiation boundary conditions will ever be available in HZETRN. We use the latest JSC cosmic-ray model[38]. Special numerical procedures have been developed to assure accuracy of HZETRN in LEO due to spectral discontinuities caused by the geomagnetic cutoffs. HZETRN can never be tested in the laboratory since highly specialized numerical procedures are required for such high energy resolution beams in the lab but not in space. This energy resolution problem is true for any numerical difference procedure as well. Only laboratory-like boundary conditions are presently available in GRNTRN. Once GRNTRN receives space boundary conditions, no new numerical problems arise as GRNTRN is an analytic solution with unlimited energy resolution.

5. APPLICATIONS TO SPACE RADIATION ISSUES

The exposure of astronauts to space radiation presents many challenges in understanding the harmful effects of ionizing radiation, such as assessing the importance of track structure for relativistic ions which have large lateral extension from the production of secondary electrons (delta rays). There are also the effects of protraction of the radiation exposure which may lead to enhancements in biological effects for high LET radiations[39] and sparing in many cases for low LET ions. Because the biological effects of HZE radiations are uncertain at this time, the experimental studies in the laboratory and in space with cell cultures and animals will undoubtedly continue. Several studies are already completed, which are discussed in the reports

of the National Council of Radiation Protection[39,40]. It is now well established in experiments with multiple ion beams that the biological response depends on the specifics of the distribution of energy about the ion path in addition to LET as it passes through the sensitive structures of biological cells. Biophysical models with phenomenological enzymatic repair processes have been used to describe the cellular response for several biological endpoints[41,42,5]. The understanding of the biological response of test systems will unavoidably depend on the detailed characteristics of the high-energy radiation as it passes through the spacecraft materials and the biological tissues and organs.

The codes have also been applied to study the single event upset rates in the shuttle computers. Just as we found it necessary to account for the specific detector response in understanding the D1 data in fig. 4, a similar attention to detail is required to understand the effects on the SEU rates. In the case of SEU, we not only treat the distribution of upset sensitivity within the device elements but must allow for the longitudinal and lateral characteristics of the track structure and Auger recombination within the track[6]. Results of such improvements are shown in table 1. In addition to the improvement in the absolute rates of SEU on STS-51 and STS-56, the ratio of the rates in these high (STS-56) and low (STS-51) inclination orbits.

Table 1. Comparison of Flight Data and Analyses for SEU Rates
(upsets per day per computer)

	Flight Data	Previous Analysis	This Work
STS-51	2.13	1.33	1.52
STS-56	6.05	6.26	5.85

The Langley Stratospheric Aerosol and Gas Experiment-III (SAGE-III) instrument has been designed to incorporate a claibrated CCD (charged-coupled device) as the primary spectrometer detector. Such detectors are known to be sensitive to the high-energy radiation in low-Earth orbit. An evaluation of the long-term degradation of the CCD in a shielded environment was necessary to estimate useful operation during the projected mission duration. First, Langley developed a radiation environmental model for the instrument to define the spectral high-energy particle fluences for the proposed 5-yr mission at the appropriate orbital conditions. Next, a detailed CAD (computer-aided design) model of the instrument, as shown in fig. 6, was developed in order to accurately define the structural configuration of the shielding provided by the instrument package. Finally, the Langley radiation transport codes were used in conjunction with the CAD model to predict the directional radiation flux including the transmitted primary radiations and the secondary radiations produced within the surrounding sturctures and arriving at the detector location. It was found in these studies that the neutrons produced in a titanium shield designed to protect the CCD array were damaging by producing displacement damage in the CCD active volume resulting in unacceptable performance. Replacement with an aluminum shield element was sufficient to reduce the neutron component allowing adequate shielding and reducing the weight of the overall instrument. Further work to characterize the signal in the array by passing charged particles are being studied using the delta ray codes and it appears that these spurious signals can be predicted but could also be analyzed to identify the particle causing the track.

6. REFERENCES

1. J. W. Wilson, L. W. Townsend, W. Schimmerling, G. S. Khandelwal, F. Khan, J. E. Nealy, F. A. Cucinotta, L. C. Simonsen, J. L. Shinn, and J. W. Norbury, "Transport Methods and Interactions for Space Radiations." *NASA RP-1257*, 1991.

2. J. W. Wilson, S. Y. Chun, F. F. Badavi, L. W. Townsend, and S. L. Lamkin, "HZETRN: A Heavy Ion/Nucleon Transport Code for Space Radiations." *NASA TP-3146*, 1991.

3. J. L. Shinn and J. W. Wilson, "Nuclear Reaction Effects in Use of Newly Recommended Quality Factor." Health Physics, Vol. 61, 1991.

4. F. A. Cucinotta, R. Katz, J. W. Wilson, and R. R. Dubey: "Heavy Ion Track-Structure Calculations for Radial Dose in Arbitrary Materials." *NASA TP-3497*, 1995.

5. F. A. Cucinotta, J. W. Wilson, M. R. Shavers, and R. Katz, "Effects of track structure and cell inactivation on the calculation of heavy ion mutation rates in mammalian cells." Int. J. Radiat. Biol., Vol. 60, No. 5 pp. 593–600, 1995.

6. J. L. Shinn, F. A. Cucinotta, J. W. Wilson, G. D. Badhwar, P. M. O'Neill, and F. F. Badavi, "Effects of Target Fragmentation on Evaluation of LET Spectra From Space Radiations in Low-Earth Orbit (LEO) Environment: Impact on SEU Predictions." IEEE Trans. Nucl. Science, Vol. 42, pp. 2017–2025, 1995.

7. W. Schimmerling, M. Rapkin, M. Wong, and J. Howard, "The Propagation of Relativistic Heavy Ions in Multi-Element Beam Lines." Med. Phys. 13: 217–228.

8. J. W. Wilson and G. S. Khandelwal, "Proton Dose Approximation in Arbitrary Convex Geometry." Nuclear Technol. 23, pp. 298–305, 1974.

9. J. J. Lambiotte, J. W. Wilson, and T. A. Filippas, "Proper 3C: A Nucleon Pion Transport Code." *NASA TM X-2158*, 1971.

10. R. Singleterry, "Development of deterministic transport methods for low energy neutrons for shielding in space." Ph.D. Diss., University of Arizona, 1993.

11. J. W. Wilson and S. L. Lamkin, "Perturbation Theory for Charged Particle Transport in One Dimension." Nucl. Sci. and Eng. Vol. 57, 292, 1975.

12. J. W. Wilson, Y. J. Xu, E. Kamaratos, and C. K. Chang, "Mean Excitation Energies for Stopping Powers in Various Materials Composed of Elements Hydrogen Through Argon," Canadian J. Physics, Vol. 62, pp. 646–660, 1984.

13. J. L. Shinn, H. Farhat, F. F. Badavi, and J. W. Wilson, "Polarization Correction for Ionization Loss in a Galactic Cosmic Ray Transport Code (HZETRN)." *NASA TM 4443*, 1993.

14. J. W. Wilson, M. Kim, W. Schimmerling, F. F. Badavi, S. A. Thibeault, F. A. Cucinotta, J. L. Shinn, and R. Kiefer: "Issues in Space Radiation Protection: Galactic Cosmic Rays." Health Phys. 68: 50–58; 1995.

15. M. E. Rudd, "User-Friendly Model for the Energy Distribution of Electrons from Proton or Electron Collisions." Nucl. Inst. Meth. 16: 213–218; 1989.

16. G. Depouy, F. Perrier, and F. Arnal: Compt. Rend. Acad. Sci. (Paris) 258: 3655; 1964.

17. E. J. Kobetich and R. Katz, "Width of Heavy-Ion Tracks in Emulsion." Phys Rev. 170: 405–411; 1968.

18. F. A. Cucinotta, L. W. Townsend, and J. W. Wilson, "Model of Alpha-Nucleus Interaction Cross Sections." *NASA TP-3285*, 1993.

19. F. A. Cucinotta and R. R. Dubey, "Final-State Interactions and Inclusive Nuclear Collisions." *NASA TP-3353*, August 1993.

20. L. W. Townsend, J. W. Wilson, F. A. Cucinotta, and J. W. Norbury, "Comparison of Abrasion-Model Differences in Heavy Ion Fragmentation: Optical Versus Geometric Models." Phys. Rev. C 34, pp. 1491–1494, 1986.

21. J. W. Wilson, L. W. Townsend, B. D. Ganapol, S. Y. Chun, and W. W. Buck, "Charged Particle Transport in One Dimension." Nucl. Sci. and Eng. 99, 285, 1988.

22. J. W. Wilson, L. W. Townsend, H. H. Bidasari, W. Schimmerling, M. Wong, and J. Howard, "20Ne Depth-Dose Relations in Water," Health Phys. 46:1101–1111; 1984.

23. J. W. Wilson, L. W. Townsend, and F. F. Badavi, "A Semiempirical Nuclear Fragmentation Model," *Nucl. Inst. & Meth. Phys. Res. B18*, 225, 1987.

24. J. W. Wilson, "Analysis of the Theory of High-Energy Ion Transport," *NASA TN D-8381*, 1977.

25. J. W. Wilson and F. F. Badavi, "New Directions in Heavy Ion Transport." In Proceedings of "*New Horizons in Radiation Protection and Shielding*," p. 205, ANS, Le Grange Park, IL, 1992.

26. J. W. Wilson, L. W. Townsend, J. L. Shinn, F. A. Cucinotta, R. C. Costen, F. F. Badavi, and S. L. Lamkin, "Galactic Cosmic Ray Transport Methods: Past, Present, and Future." Adv. in Sp. Res., Vol. 14, No. 10, pp. 841–852, 1994.

27. S. Y. Chun, G. S. Khandelwal, J. W. Wilson, "A Green's Function Method for High Charge and Energy Ion Transport." Nucl. Sci. and Eng. 122: 267–275; 1996.

28. C. J. Zeitlin, K. A. Frankel, W. Gong, L. Heilgronn, E. J. Lampo, R. Leres, J. Miller, and W. Schimmerling: "A Modular Solid State Detector for Measuring High Energy Heavy Ion Fragmentation Near the Beam Axis." Radiat. Meas. 23: 65–81; 1994.

29. J. W. Wilson, R. K. Tripathi, F. A. Cucinotta, J. L. Shinn, F. F. Badavi, S. Y. Chun, J. W. Norbury, C. J. Zeitlin, L. Heilbronn, and J. Miller: "NUCFRG2: An evaluation of the semiempirical nuclear fragmentation database." *NASA TP-3325*, 1995.

30. J. L. Shinn, J. W. Wilson, W. Schimmerling, M. R. Shavers, J. Miller, E. V. Benton, A. L. Frank, and F. F. Badavi, "A Green's Function Method for Heavy Ion Beam Transport." Radiat. Environ. Biophys., 34, pp. 155–159, 1995.

31. G. D. Badhwar, J. U. Patel, F. A. Cucinotta, and J. W. Wilson, "Measurements of the Secondary Particle Energy Spectra in the Space Shuttle." Radiat. Meas. 24: 129–138; 1995.

32. F. A. Cucinotta, L. W. Townsend, J. W. Wilson, J. L. Shinn, G. D. Badhwar, and R. R. Dubey: "Light Ion Components of the Galactic Cosmic Rays: Nuclear Interactions and Transport Theory." Presented at the COSPAR XXX Plenary Meeting, Hamburg, Germany, July 11–21, 1994. Advances in Space Research, Vol. 17, No. 2, pp. (2)77–(2)–86, 1996.

33. B. Weigel, W. Heinrich, E. V. Benton, and A. Frank: "Measurements of LET Spectra and Comparison to Models." Adv. Space Res. 12: 3349–354; 1992.

34. J. W. Wilson, J. L. Shinn, L. W. Townsend, R. K. Tripathi, F. F. Badavi, and S. Y. Chun: "NUCFRG2: A Semiempirical Nuclear Fragmentation Model." Nuclear Instruments and Methods in Physics Research, Part B Vol. 94 (1994) pp. 95–102.

35. J. R. Letaw et al., "Radiation hazards on space missions outside the magnetosphere." Adv. Space Res. 9(10): 285–291; 1989.

36. J. W. Wilson, L. W. Townsend, and F. F. Badavi, "Galactic HZE Propagation Through the Atmosphere," Radiat. Res. 109, 173, 1987.

37. R. Silberberg, C. H. Tsao, and M. Shapiro, "Semiempirical Cross Sections and Applications to Nuclear Interactions of Cosmic Rays," *Spallation Nuclear Reactions and Their Applications*, B. S. P. Shen and M. Merker, eds., pp. 49–81 eds., Reidel Publishing Co., 1976.

38. G. D. Badhwar, F. A. Cucinotta, and P. M. O'Neill, Depth-Dose Relationships for Cosmic Rays at Various Solar Minima., Radiat. Res., 134, pp. 9–15, 1993.

39. Anon., The Relative Biological Effectiveness of Radiations of Different Quality. National Council on Radiation Protection and Measurements, *NCRP Rep. 104*, 1990.

40. Anon., Guidance on Radiation Received in Space Activities. National Council•on Radiation Protection and Measurements, *NCRP Rep. 98*, 1989.

41. J. W. Wilson, F. A. Cucinotta, and J. L. Shinn, "Cell Kinetics and Track Structure." *Biological Effects and Physics of Solar and Galactic Cosmic Radiation*, C. E. Swenberg, G. Horneck, and E. G. Stassinopoulos, eds., pp. 295–338, Plenum Press, 1993.ar

42. F. A. Cucinotta, J. W. Wilson, R. Katz, W. Atwell, and G. D. Badhwar: 'Track Structure and Radiation Transport Models for Space Radiobiology Studies." Adv. in Space Res., 17, 1995.

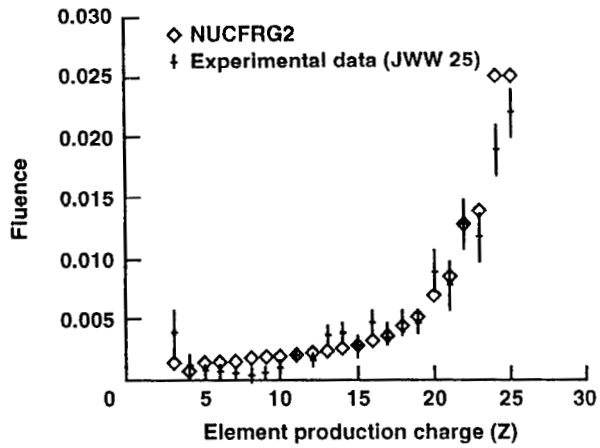

Figure 1. Charge removal cross sections for Fe ions at 600 A MeV in polyethylene.

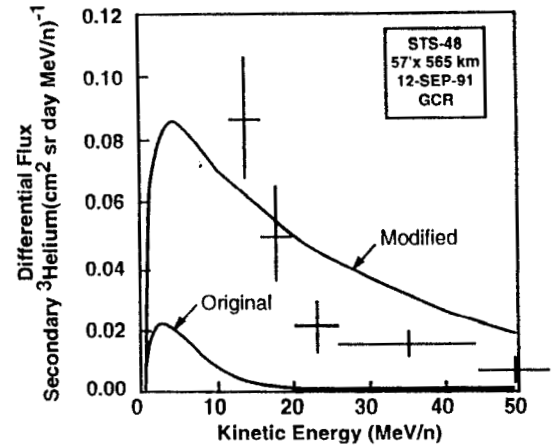

Figure 2. A plot of the differential energy spectrum of secondary ^{3}He produced by GCR particles in STS-48. The solid curves are due to HZETRN model calculations.

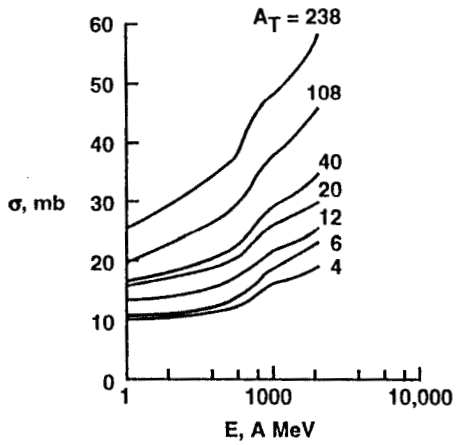

Figure 3. Alpha knockout cross section leaving a ground state ^{12}C core.

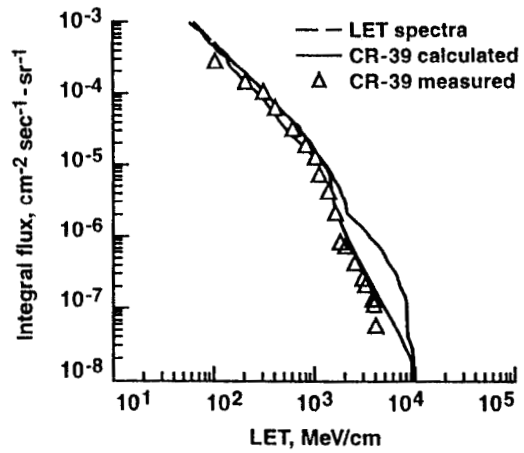

Figure 4. Calculated LET spectra, predicted CR-39 response, and measured CR-39 response for the DI mission.

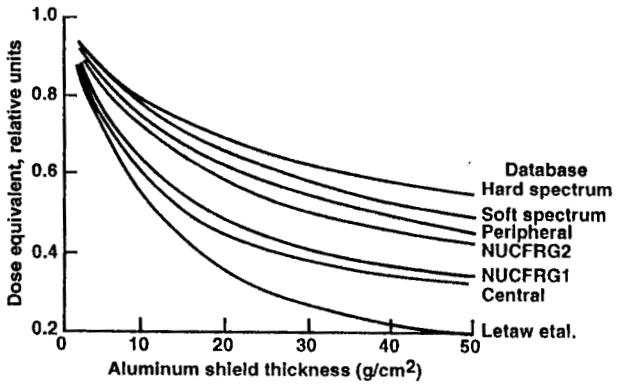

Figure 5. Shield attenuation for solar minimum galactic cosmic ray dose equivalent resulting from nuclear fragmentation models.

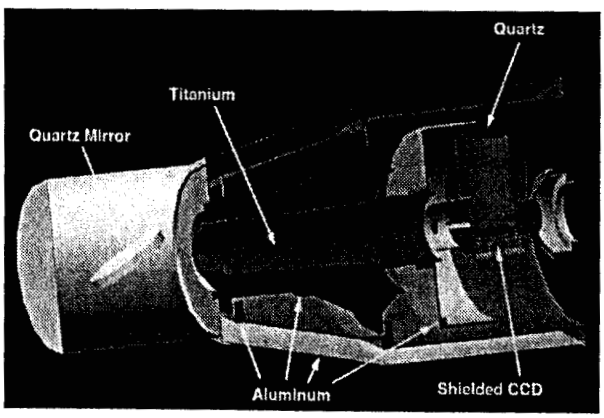

Figure 6. CAD model of SAGE-III instrument.